



Adsorptive removal of copper (II) from aqueous solutions using low cost Moroccan adsorbent. Part I: Parameters influencing Cu(II) adsorption

Khaled C. Nebagha^a, Khadija Ziat^{a*}, Lotfi Rghioui^{b,c}, Mohamed Khayet^{d,e}, Mohamed Saidi^a, Khadija Aboumaria^f, Abderrahim El Hourch^g, Said Sebti^h

^a Laboratoire Physico-Chimie des Matériaux, Substances Naturelles et Environnement, Faculty of Sciences and Techniques, Abdelmalek Essaâdi University, Tangier (Morocco).

^b Equipe Physico-Chimie de la matière condensée, Faculty of Sciences, Moulay Ismail University, Meknès (Morocco).

^c Laboratoire de Spectroscopie, Modélisation Moléculaire, Matériaux et Environnement (LS3ME), Faculty of Sciences, Mohammed V-Agdal University, Rabat (Morocco).

^d Department of Applied Physics I, Faculty of Physics, University Complutense of Madrid, Avda. Complutense s/n, 28040, Madrid (Spain).

^e Madrid Institute for Advanced Studies of Water (IMDEA Water Institute), Calle Punto Net N° 4, 28805, Alcalá de Henares, Madrid (Spain).

^f Department of Earth Sciences, Faculty of Sciences and Techniques, Abdelmalek Essaâdi University, Tangier (Morocco).

^g Equipe d'Electrochimie et Chimie Analytique, Faculty of Sciences, Mohammed V-Agdal University, Rabat (Morocco).

^h Laboratoire de Chimie Organique Catalyse et Environnement, Faculty of Sciences of Ben M'Sik, Hassan II University, Mohammedia-Casablanca (Morocco).

Received 28 Jul 2015, Revised 17 Sep 2015, Accepted 18 Sep 2015

* Corresponding author: E-mail: khadijaziat@gmail.com

Abstract

Treated Martil sand (TMS) is proposed as a mineral sorbent for removal of copper ions from aqueous solutions. TMS was characterized by different techniques such as XRF, XRD, FTIR, SEM, and BET. The effects of pH, adsorbent dosage, ionic strength, temperature, and contact time were investigated. Binding Cu(II) was found to be highly pH dependent. The thermodynamic analysis indicated that the adsorption was endothermic and the computation of the parameters, ΔH° , ΔS° and ΔG° , indicated that the interaction was thermodynamically favorable. In general, the results indicated that TMS is suitable as a sorbent material for adsorption of Cu(II) from aqueous solutions for its high effectiveness and low cost.

Keyword: Martil sand, Copper(II), Adsorption, Low cost adsorbent, Thermodynamic.

1. Introduction

Industrial wastewater treatment for the removal of pollutants such as heavy metal ions remains a worldwide challenge. Heavy metal ions discharged with industrial effluents usually find their way into receiving water bodies such as rivers, lakes and streams increasing their pollution. Copper is one of the heavy metals most toxic to living organisms and one of the most widespread heavy metals in the environment [1].

Copper pollution generally arises from copper mining and smelting, brass manufacturing, electroplating industries and excessive use of Cu-based agro-chemicals. In fact, copper is essential to human life and health, but like all other heavy metals, it is potentially toxic at high concentrations. The excessive intake of copper by Man leads to severe mucosal irritation, widespread capillary damage, hepatic and renal damage, central nervous problems followed by depression, gastrointestinal irritation and possible necrotic changes in the liver and kidney [2]. The World Health Organization recommended a maximum acceptable concentration of Cu(II) in drinking water of 1.5 mg L⁻¹ [3]. Hence, the removal of copper from aqueous solutions is extremely important.

Removing copper from large volumes of water can be technically challenging and expensive. There is a crucial need to develop a method that should be not only efficient and economical, but also easily to be implemented.

Adsorption has been found to be an effective and economic method with high potential for the removal, recovery and recycling of metals from wastewater [4]. Recently, adsorption has attracted considerable interest especially from cheap, eco-friendly and abundantly available material capable to remove significant quantities of heavy metal ions from industrial wastewater. Numerous low cost adsorbents have been used to remove

copper ions from aqueous solutions such as zeolite [5], Kaolinite and montmorillonite [6], tree fern [4], papaya wood [7] and bagasse fly ash [8].

In view of abundance of sand in several countries, use of this natural material for wastewater treatment may be of great value. In this study, the natural sand of Martil (NMS), region located at the north west of Morocco on the Mediterranean Sea, is used for the first time as adsorbent to remove copper ions from aqueous solutions. Different characterization techniques such as Fourier transform infrared spectroscopy (FTIR), X-ray diffraction (XRD), X-ray fluorescence and scanning electron microscope (SEM) were used to study the surface and functional group of this adsorbent. The effect of various parameters affecting sorption behavior such as contact time, particle size, pH of the medium, adsorbent dose, ionic strength, foreign ions and temperature has been investigated to better understand the Cu(II) adsorption process.

2. Experimental

2.1. Materials

The sea sand (NMS) used was collected from Martil Beach located at the north west of Morocco on the Mediterranean Sea. After collection, stones and other heavy particles were removed from the sample. Subsequently, the NMS was soaked in concentrated nitric acid (14.65 M) for 1h and then washed thoroughly to remove all acid. Finally, the washed sample was dried in oven at 100 °C for 24h, grounded and sieved. The obtained sample, named hereafter treated Martil sand (TMS), was sieved and the size of particles used in sorption tests was in the range: 125–300 µm.

All reagents used were of analytical grade and employed without any further purification. Aqueous solutions of copper Cu(II) at various concentrations were prepared by dissolving the appropriate amount of copper salt (CuSO₄·5H₂O) in deionized water.

2.2. Methods

2.2.1. Characterization techniques

The chemical composition of the sorbent was determined by means of X-ray fluorescence (XRF) using an Axios Spectrometer. The mineralogical composition of the sand samples was obtained by X-ray diffraction (XRD). The measurements were performed using an X'pert-Pro MPD diffractometer with Cu Kα₁ radiation ($\lambda = 1.5406 \text{ \AA}$) operating at 45 kV and 40 mA within the 2θ range of 3–90°. Data were collected with the rate of 0.067°/min at 298 K. The XRD patterns were identified by carrying out comparisons to the JCPDS standards.

Fourier transform infrared spectroscopy (FTIR) was used to determine the frequency changes in the functional groups responsible for binding Cu(II). Samples of natural sand (NMS), treated sand (TMS) or Cu(II) loaded treated Martil sand (TMS–Cu) (filtered and dried after contact with an initial Cu(II) ions concentration of 250 mg L⁻¹ at pH 4) were mixed in KBr at a ratio of 1:100 and compressed into films for FTIR analysis using a Vertex 70 spectrometer. Infrared absorbance data were recorded at room temperature in the wavenumber region 400–4000 cm⁻¹.

The surface analysis of TMS was carried out by BET method using a Quantachrome Autosorb automated nitrogen adsorption system. The N₂ surface area of TMS was found to be 1.8 m² g⁻¹.

For SEM (FEI/Quanta 200 Scanning Electronic Microscope) analysis, the samples were coated with thin carbon film in order to avoid the influence of charge during the SEM operation.

The surface charge characteristics of NMS and TMS samples were measured by potentiometric titration. Suspensions of NMS or TMS were prepared by mixing with a magnetic stirrer 0.5 g of solid sample with 50 mL of NaCl at different ionic strengths (10⁻¹, 10⁻², 10⁻³ M). The pH value was adjusted by adding 0.1 M HCl solutions. The suspension was then titrated by the addition of 0.1 M NaOH solution. The pH was recorded after five minutes of each addition of a small amount of base (0.2 mL). To check reversibility process, the suspension was back-titrated with 0.1 M HCl solution as it was reported elsewhere [9].

2.2.2. Adsorption experiments

Adsorption equilibrium experiments were conducted at room temperature by equilibrating an accurately weighed 5 g TMS with 25 mL of copper ion solution at concentration of 250 mg L⁻¹. The mixture was agitated for 10 h to assure the adsorption equilibrium. The solid was separated by centrifugation and the filtrate was analyzed by a flame atomic absorption spectrophotometer (Jobin Yvon 2) to determine the residual copper concentration. The effect of pH on Cu(II) adsorption was studied at various initial pH values ranging between 1–5 with a fixed amount of adsorbent (5 g) and initial Cu(II) concentration of 250 mg L⁻¹.

The pH of the solutions was adjusted by adding 0.1 M HNO₃ or 0.1 M NaOH. The effect of the adsorbent dose was conducted by varying the adsorbent amounts from 0.5 to 7 g with Cu(II) ions concentration of 250 mg L⁻¹ at pH 4. The effect of the ionic strength on the amount of copper adsorbed from solution containing NaNO₃ and Ca(NO₃)₂ in the concentration range of 0.001–1.0 M was studied at room temperature.

The percentage removal of copper ions and the adsorption capacity of the adsorbent at equilibrium, q_e (mg g⁻¹), were calculated using the following equations:

$$\% \text{ Adsorption} = \frac{(C_0 - C_e)}{C_0} \times 100 \quad (1)$$

$$q_e = \frac{(C_0 - C_e)V}{m} \quad (2)$$

where C_0 and C_e (mg L⁻¹) are the initial and equilibrium concentration of copper ion solution respectively, V is the volume of the solution (L) and m is the amount of adsorbent used (g).

2.2.3. Thermodynamic study

In order to obtain the thermodynamic nature of the adsorption process, 5g TMS was added into 25 mL Cu(II) solutions with an initial concentration of 250 mg L⁻¹ at different temperatures (303, 313, 323 and 333 K). Thermodynamic parameters, namely, standard Gibbs free energy (ΔG°), standard enthalpy (ΔH°) and standard entropy (ΔS°) changes were also determined from the experimental data at different temperatures using the following equations [10]:

$$\ln K_d = \frac{\Delta S^\circ}{R} - \frac{\Delta H^\circ}{RT} \quad (3)$$

$$K_d = \frac{V}{m} \frac{C_0 - C_e}{C_e} \quad (4)$$

where K_d is the distribution coefficient for the adsorption (mL g⁻¹), R is the ideal gas constant (8.314 J mol⁻¹ K⁻¹) and T is the absolute temperature of the aqueous solution. The values of ΔH° and ΔS° were obtained from the slope and intercept of $\ln K_d$ versus $1/T$ plots.

After obtaining ΔH° and ΔS° values of the adsorption, ΔG° of each temperature was calculated by the well-known equation as follows:

$$\Delta G^\circ = \Delta H^\circ - T\Delta S^\circ \quad (5)$$

3. Result and discussion

3.1. Characterization of Martil sand

3.1.1. Sand particle distribution

Particle size analysis was performed on decalcified samples and treated with oxygenated water after dry sieving for 20 min using a thirteen column screen type AFNOR. Approximately, 1 kg of prepared sand was passed through these sieves. The Collected fractions of particle sizes were weighted using electronic balance (Model: Precisa 6200 D). Figure 1 shows the grain size distribution by plotting the class weight versus the particles diameter. The particles are predominantly in the range of 250–300 μm indicating that NMS is a medium one. In the present study, three particle size ranges: 125–180 μm , 180–250 μm and 250–300 μm were selected to find the optimum range for adsorption of copper (II).

3.1.2. SEM analysis

SEM images of NMS, TMS and TMS after Cu(II) adsorption (TMS-Cu) are presented in Fig. 2. The SEM image of the NMS showed platelet morphology with irregular rough structure (Fig. 2a). After acid treatment, the morphology of sand changed into uniform structure shape with creation of inter-granular porosity, which is due to the disappearance of calcite and dolomite phases after acid treatment (Fig. 2b). After adsorption of copper, the surface becomes smooth with disappearance of the intergranular porosity as shown in Fig. 2c.

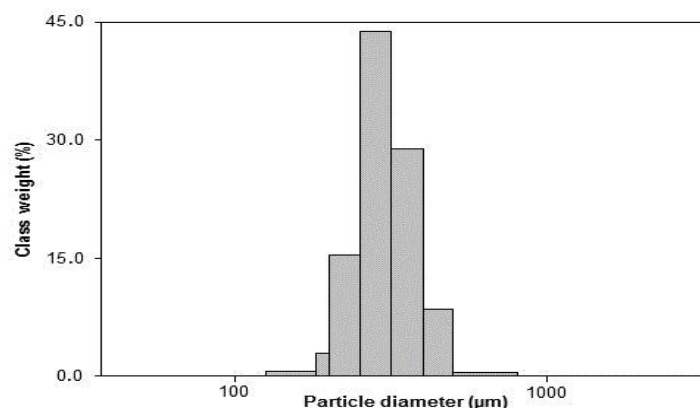


Figure 1: Grain size distribution of NMS.

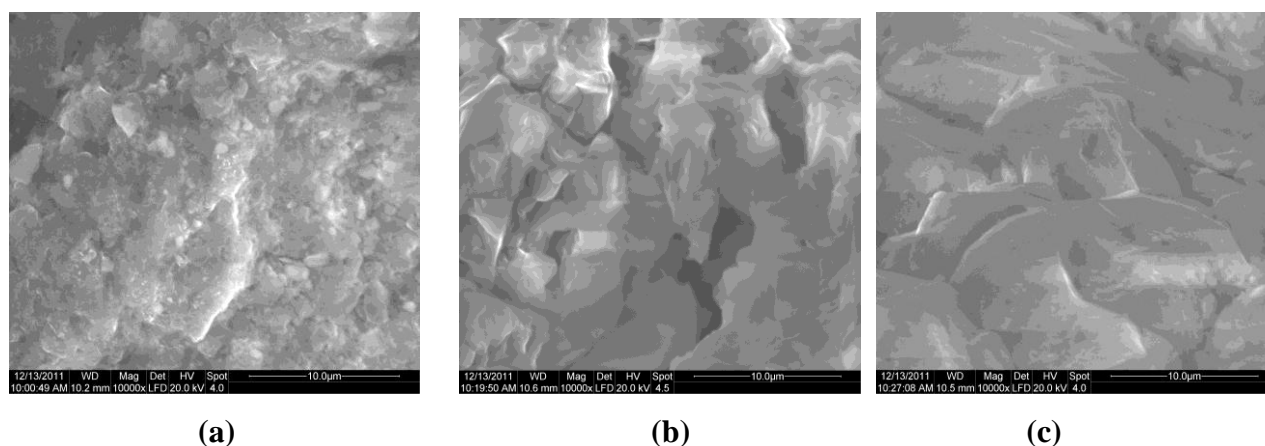


Figure 2: SEM images of Martil sand (a: NMS; b: TMS; c: TMS–Cu) taken at x 10,000 magnifications.

3.1.3. XRF and XRD studies

As it was stated previously, the chemical composition of TMS in weight percentage of oxides was determined by XRF. The results are as follows: SiO₂ (86.5), Al₂O₃ (4.1), Fe₂O₃ (3.61), Cr₂O₃ (1.75), Na₂O (1.06), MgO (0.554), WO₂ (0.45), K₂O (0.313), SO₃ (0.189), CaO (0.185), MnO₂ (0.158).

The X-ray diffractograms of NMS, TMS and TMS-Cu are presented in Fig. 3. The diffractogram of NMS showed that the dominant phase is the quartz SiO₂ (JCPD pattern n° 01-085-0457) with the presence of calcite CaCO₃ (JCPDS pattern n° 01-083-0578), dolomite CaMg(CO₃)₂ (JCPDS pattern n° 01-036-0426) and muscovite KAl₂Si₃AlO₁₀(OH)₂ (JCPDS pattern n° 01-007-0032). After treatment, quartz and muscovite were maintained, while calcite and dolomite disappeared. No significant changes were observed after copper adsorption in the diffractogram of TMS-Cu.

3.1.4. FTIR characterization

Figure 4 shows the infrared spectra of NMS, TMS and TMS-Cu. It can be observed that the three spectra are divided into two sections. The first one comprises the main sharp distinctive and characteristic absorption bands extending in the region from 400 to about 1450 cm⁻¹, and the second part is located from 3400 to 3700 cm⁻¹, which reveals one peak around 3624 cm⁻¹ and a broad band centered at about 3430 cm⁻¹.

It is evident that the part of spectrum between 400 to 1400 cm⁻¹ corresponds to the absorption due to main silicate and carbonate network group's vibrations with different bonding arrangement, and the rest of the spectrum from 1400 to 4000 cm⁻¹ is obviously consisting of vibrations due to water and silanol group (Si–Si–OH).

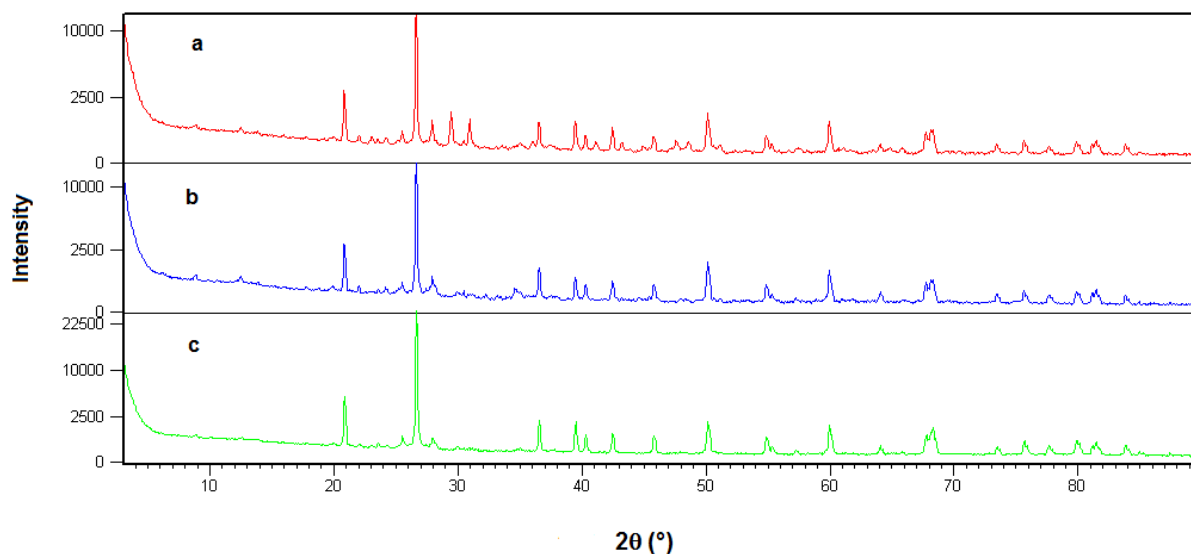


Figure 3: XRD patterns of Martil sand (a: NMS; b: TMS; c: TMS-Cu).

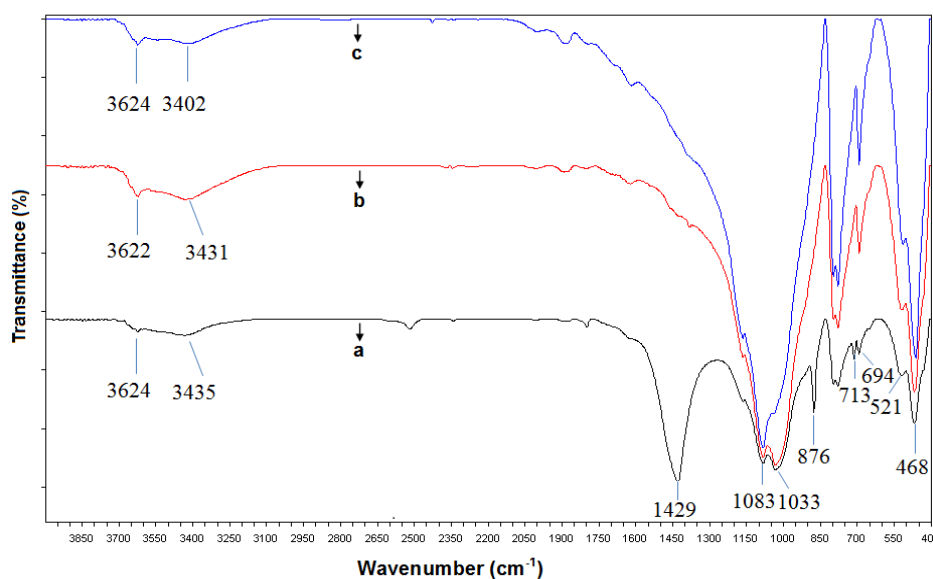


Figure 4: Infrared spectra of Martil sand (a: NMS; b: TMS; c: TMS-Cu).

According to other studies [10-15], the band assignments are given in Table 1. The absorption band at 3624 cm^{-1} is assigned to the stretching modes of the Si–Si–OH group [11]. The broad band at about 3430 cm^{-1} corresponds to the O–H stretching vibration [12,13]. The strongest band observed at 1429 cm^{-1} in the infrared spectrum of NMS (Fig. 4a) is associated with the stretching vibration of carbonate groups (CO_3^{2-}). The corresponding deformation vibration is observed at 876 cm^{-1} [12]. These two bands disappear in the infrared spectrum of the TMS due to the action of the acid (Fig. 4b). Similar results were obtained for natural Jordanian sorbent after treatment with nitric acid [16].

The peak around 1083 cm^{-1} is attributed to the asymmetrical vibration modes of the Si–O bond in the tetrahedral SiO_4 unit of SiO_2 matrix [14]. The band located at 1033 cm^{-1} confirms that the Si atom is in a tetrahedral sheet [10]. This peak was found to shift from 1033 to 1042 cm^{-1} after copper adsorption. The four or three bands observed in the spectra between 800 and 690 cm^{-1} are attributed to the Si–O of quartz and M–O stretching vibration (M = Fe, Al, ...). It must be pointed out that O–Si–O, Si–O–Si and Si–O–Al bending modes show absorption bands at 460 cm^{-1} and 510 cm^{-1} [15–17].

According to IR spectra of NMS and TMS, it is obvious that the frequency bands are not affected by acid treatment (Table 1). This indicates that the acid treatment had no effect on the structure of silicate materials present in the adsorbent. The comparison of the TMS and TMS-Cu spectra shows that the vibrations of O–H and Si–O groups are sensitive to the sorption reaction. In fact, a remarkable shift of their wavenumbers vibrations is observed. The shift in wavenumber of O–H and Si–O vibrations groups corresponds to the change in energy of the functional group, indicating the change of the bonding pattern of O–H and Si–O groups after adsorption. These results confirm the involvement of these groups in Cu(II) binding for TMS.

The shift of the vibration band of O–H group to the lower wavenumbers after copper adsorption implies a decrease of the force constant of the bond, which reduces the covalent binding of O–H. Regarding the vibration band of Si–O, the opposite phenomenon was observed. In fact, the wavenumber of the vibration of this band was found to increase after copper sorption indicating an enhancement of the covalent binding of Si–O.

Table 1: Infrared wavenumbers of Martil sand vibrations (cm⁻¹) and their attributions.

Wavenumber (cm ⁻¹)			Functional group assignment
NMS	TMS	TMS-Cu	
3624	3622	3624	Si–Si–O–H
3435	3432	3402	O–H
1429			CO ₃ ²⁻
1169	1169	1169	Si–O
1083	1082	1083	
1033	1033	1042	
876			CO ₃ ²⁻
Doublet { 797 779	800 779	797 779	Si–O and M–O
Doublet { 713 694	– 693	– 693	
521	519	510	O–Si–O
468	468	462	Si–O–Si

3.1.5. Point of zero charge (PZC)

The point of zero charge (PZC) is defined as the pH value for which the surface charge of the sample is equal to zero. The surface charge is calculated from the potentiometric titration curves according to the relationship:

$$\sigma_H = \frac{F(C_a - C_b + [OH^-] - [H^+])}{mS} \quad (13)$$

where σ_H is the surface charge density (C m⁻²), F the Faraday constant (C mol⁻¹), C_a and C_b are the concentrations (mol L⁻¹) of the acid and base added to the suspension, [OH⁻] and [H⁺] are the concentration of OH⁻ and H⁺ measured from the pH of the solution, m is the mass of the solid sample in the solution (g L⁻¹), and S is the specific surface area of the sample (m² g⁻¹).

Figure 5 shows the pH effect on the surface charge density of NMS and TMS at different NaCl concentrations. It can be seen that, for all NaCl concentrations, the surface charge density is zero at a pH value of 11.3 for NMS while it is 3.3 for TMS. The high value of PZC of NMS is due to the presence of carbonate groups as calcite and dolomite. The PZC of calcite lies within the range of pH 8 to 10.8 [18,19]. The high value of PZC of NMS is due to the presence of carbonate groups as calcite and dolomite. The PZC of calcite lies within the range of pH 8 to 10.8 [18,19]. The surface charge of calcite depends on the electrolyte medium, the type of material, and pH adjustment (i.e., acid/base solution or CO₂ pressure) [20]. It is also influenced by the presence of other minerals. The PZC of TMS is slightly higher than that reported in the literature for pure quartz (2.9) [21]. This could be explained by the presence of muscovite in the TMS. A similar effect has been reported for the beach sand taken from Hawks Bay (Karachi, Pakistan) by Taqvi et al. [22]. A similar effect has been reported for the beach sand taken from Hawks Bay (Karachi, Pakistan) by Taqvi et al. [22].

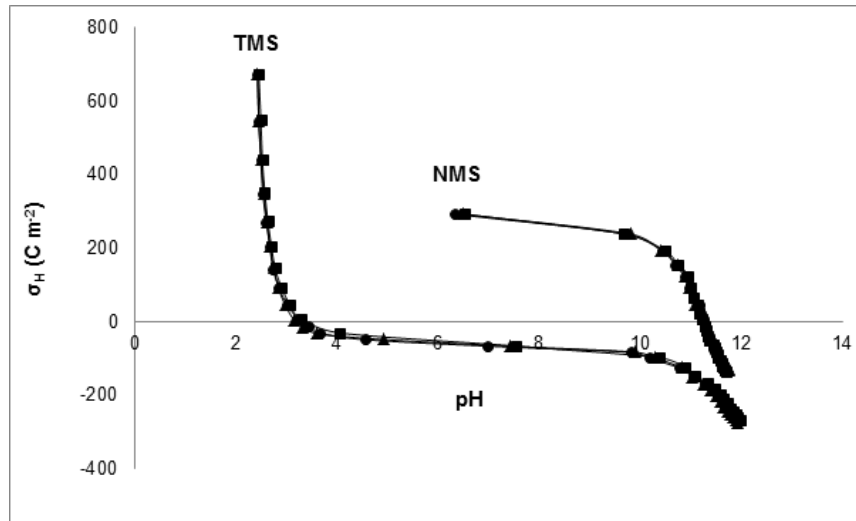


Figure 5: Surface charge density vs. pH curves of NMS and TMS in NaCl solutions: ●, 0.1 M; ■, 0.01 M and ▲, 0.001 M (T: room temperature, $m = 0.01 \text{ g mL}^{-1}$).

3.2. Factors affecting Cu(II) adsorption

3.2.1. Particle size and contact time

To investigate the effect of contact time on copper uptake, a series of experiments have been performed at a constant initial Cu(II) concentration (C_0) of 250 mg L^{-1} , $\text{pH} = 4.0$ and various TMS particle sizes. Figure 6 shows the Cu(II) adsorption with time. As it can be seen, the particle size has a significant influence on copper sorption. As observed, the particle size has a significant influence on copper sorption. The increasing grain size led to the loss of sand ability to bind Cu(II). The extent of adsorption increases as the particle size decreases. This may be due to the enhanced surface area available for the adsorption. A similar phenomenon was reported previously for other adsorbents [23, 24]. The Cu(II) uptake is rapid during the first hour after which equilibrium is slowly achieved. Almost 70 % of total removal of Cu (II) is occurred within 1h. Adsorption equilibrium was reached in 8 h and no remarkable changes were observed for longer contact time. The initial sorption profile of TMS-Cu as a function of the time could be explained on the basis that, in the initial stage of sorption, a large number of vacant surface sites are available for adsorption. Hence, the amount of copper adsorbed was increased rapidly and then, the remaining vacant surface sites were difficult to be occupied because of the repulsive forces between the copper cations on TMS and the bulk phase. Based on these results, the particle size range 125–180 μm was selected for the subsequent experiments.

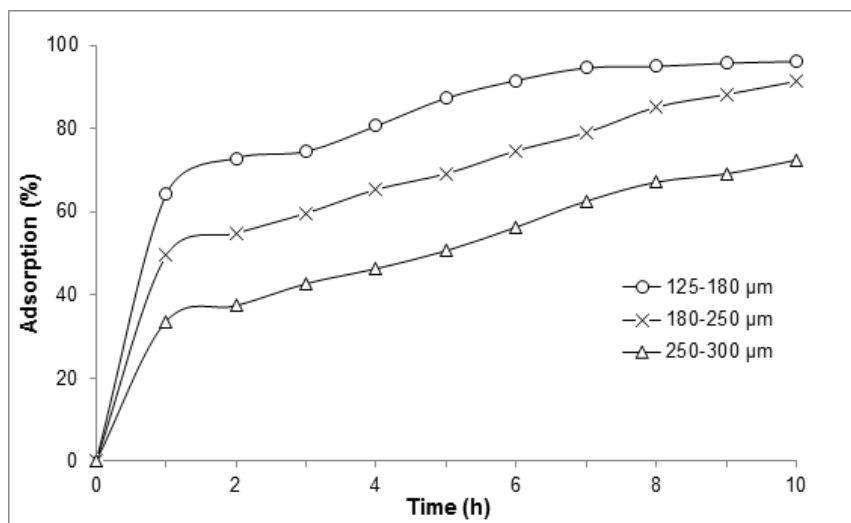


Figure 6: Effect of particle size on copper sorption by TMS (T: room temperature, $C_0 = 250 \text{ mg L}^{-1}$, $\text{pH} = 4.0$, and $m = 0.2 \text{ g mL}^{-1}$).

3.2.2. Effect of pH

The effect of pH on the removal of Cu(II) ions from solution was investigated by varying the pH of metal solution within the range of 1–5. The results are plotted in Fig. 7. The adsorption of Cu(II) depends on the pH value. There is a gradual enhancement of the Cu(II) adsorption with the increase of pH from 1 to 5. The Cu(II) removal efficiency increased from 50 % to 79.4 % when the pH rises from 1 to 5.

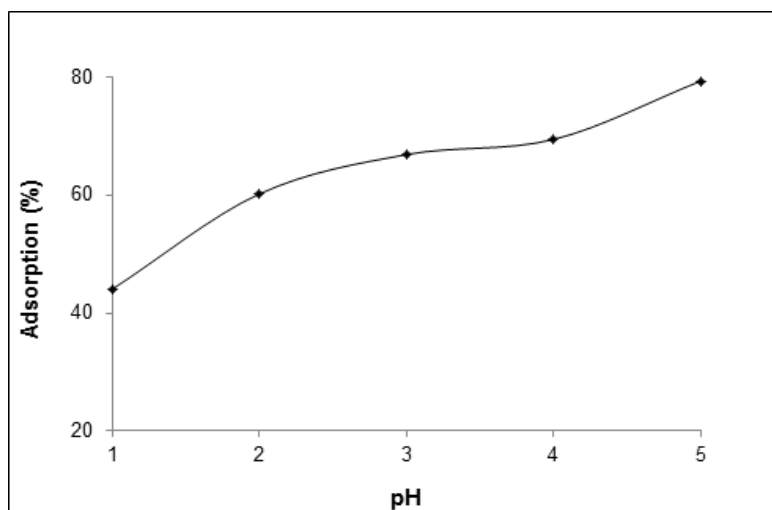


Figure 7: Effect of pH on the Cu(II) adsorption by TMS (T : room temperature, $C_0 = 250 \text{ mg L}^{-1}$, and $m = 0.2 \text{ g mL}^{-1}$).

At low pH values, Cu(II) removal were inhibited possibly due to a competition between protons and copper ions on the sorption sites. As the pH value was increased, the negative charge density on TMS surface increased due to deprotonation of the metal binding sites resulting in an increase of the adsorption of metal ions. The high dependence on the pH for Cu(II) adsorption could be explained on the basis of surface charge density of Si–O and O–H groups. As it was observed in Fig. 4c, these groups are participating in the Cu(II) adsorption as the peaks of the bands corresponding to these groups shift when TMS was loaded with Cu(II) ions as it was explained earlier.

The increase of the Cu(II) removal using TMS mainly depends upon the mixed effect of sorbing species and the surface properties of the adsorbing solid material. Regarding the PZC of TMS (i.e. $PZC = 3.3$), in a solution having a pH value lower than this PZC value, the surface of TMS is positively charged and the adsorption of metal cations could possibly take place via non-electrostatic interaction. Regarding the PZC of TMS (i.e. $PZC = 3.3$), in a solution having a pH value lower than this PZC value, the surface of TMS is positively charged and the adsorption of metal cations could possibly take place via non-electrostatic interaction.

The removal of copper ions could, therefore, be the result of the ion exchange and surface complexation phenomenon occurring on the surface of the TMS.

3.2.3. Adsorbent dose

The effect of the adsorbent dose on the equilibrium adsorption of copper ions from aqueous solution onto TMS was also studied and the results are shown in Fig. 8. From this figure, it can be observed that the adsorption of Cu(II) increased from 11.4 % to 72.5 % with an increase of the adsorbent dose from 0.5 to 5 g. This can be explained by the more availability of surface sites with the increase of the adsorbent dose. Jung et al., [25] attributed the similar behavior to the fact that the surface complexation is the major mechanism in the sorption process. It must be pointed out that the increase of the TMS dose from 5.0 to 7.0 g didn't lead to any significant change of the Cu(II) adsorption. However, the adsorption density (i.e. the amount adsorbed per unit mass) decreased as the adsorbent dose was increased. The decrease in adsorption density is mainly due to the unsaturation of adsorption sites through the adsorption reaction. It could be also attributed to the aggregation of adsorbent particle, resulted from high sorbent concentration, which would lead to a decrease in the total surface area of the sorbent and an increase in diffusional path [26]. The particle interaction brought about at high sorbent concentrations may also desorb some of the metal ions, which are loosely and reversibly bound to the sorbent surface. This result is in accordance with other similar studies on Cu adsorption [27-29]. In what follows, the adsorbent dosage was fixed at 5 g for further studies.

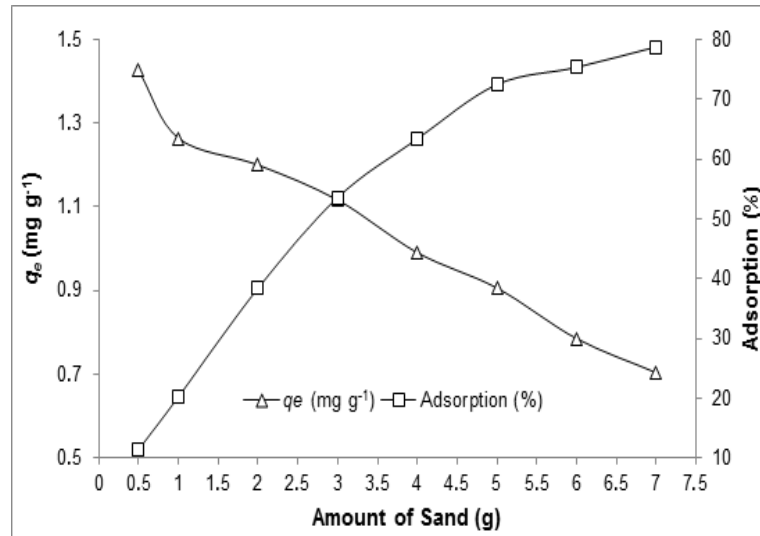


Figure 8: Effect of adsorbent dosage on the Cu(II) adsorption by TMS (T : room temperature, $\text{pH} = 4$, and $C_0 = 250 \text{ mg L}^{-1}$).

3.2.4. Ionic strength

The effect of the ionic strength on the removal of Cu(II) ions from aqueous solutions by TMS was studied. The ionic strength was adjusted using sodium nitrate (NaNO_3) and calcium nitrate ($\text{Ca}(\text{NO}_3)_2$) over the concentration range 0.001 to 1.0 mol L^{-1} . NaNO_3 and $\text{Ca}(\text{NO}_3)_2$ were added separately to copper solution. The results are shown in Fig. 9 by plotting the Cu(II) adsorption as a function of the salt concentration. The presence of NaNO_3 and $\text{Ca}(\text{NO}_3)_2$ in copper solution reduced significantly the TMS removal efficiency of Cu(II). Similar effects were reported by other authors [30,31].

The reduction of copper uptake in the presence of NaNO_3 and $\text{Ca}(\text{NO}_3)_2$ could be attributed to the competitive effect between Cu(II) and cations from the salt to occupy available sites of the adsorbent. It also suggested that increasing electrolyte concentration can cause screening of surface negative charges by the electrolyte ions leading to a drop in the adsorption of the metal ions [32]. Therefore, a decrease in the adsorption of metal ion with increasing the ionic strength of the electrolytes implies an increase of the ionic strength making the potential of the adsorbent surface less negative reducing therefore the metal ion adsorption. The presented results in Fig. 9 also showed that calcium ions had more effect on the removal of Cu(II) than sodium ions. In fact, the positive charge of Ca^{2+} is bigger than Na^+ and this may facilitate its binding to the active sites of the adsorbent. Bohn et al. [33] found that divalent metal species are generally adsorbed more readily than monovalent species.

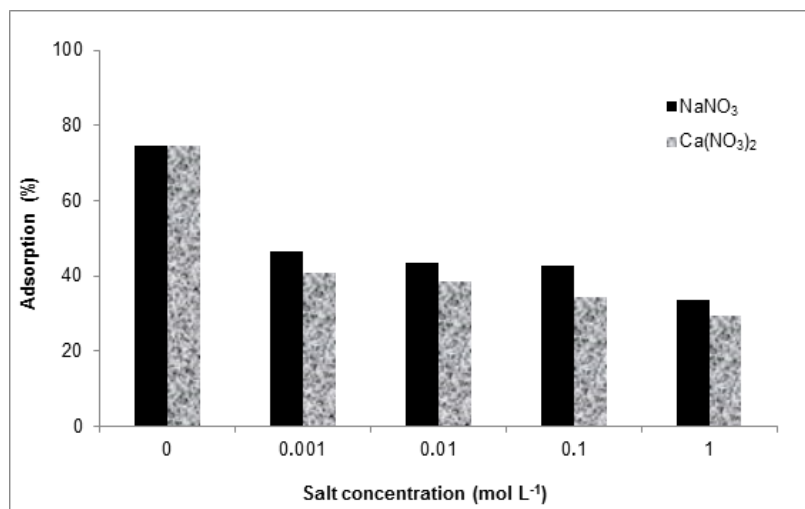


Figure 9: Effect of salt concentration on the Cu(II) sorption by TMS (T : room temperature, $\text{pH} = 4$, $C_0 = 250 \text{ mg L}^{-1}$, and $m = 0.2 \text{ g mL}^{-1}$).

3.2.5. Effect of foreign ions

Figure 10 shows the effect of foreign ions on the adsorption of Cu(II) from aqueous solution to TMS in 0.001 M LiNO₃, NaNO₃, KNO₃, NaBr and NaCl electrolyte solutions. As observed from Fig. 10a, the influence of foreign anions on the sorption of Cu(II) on TMS is the sequence of Cl⁻ > Br⁻ > NO₃⁻. The inorganic acid radicals radium order is Cl⁻ < Br⁻ < NO₃⁻ [34], the smaller radium negative charged inorganic acid radicals may form complexes with the oxygen-containing functional groups on the surfaces of TMS and thereby results in the decrease of Cu(II) sorption. The decreased amount of adsorbed Cu(II) in the presence of foreign anions can be also explained by the formation of soluble copper complexes.

From Fig. 10b, it can be seen that the sorption of Cu(II) on TMS is influenced by the suspended cations. The order of Cu(II) uptake was found to be lowest for potassium and highest for lithium, which is the order of their radii of hydration: K⁺ = 2.32, Na⁺ = 2.76 and Li⁺ = 3.4 Å [35]. The radius of K⁺ is smaller than those of the other two cations and therefore the influence of K⁺ on Cu(II) sorption is more obvious than the influences of Na⁺ and Li⁺.

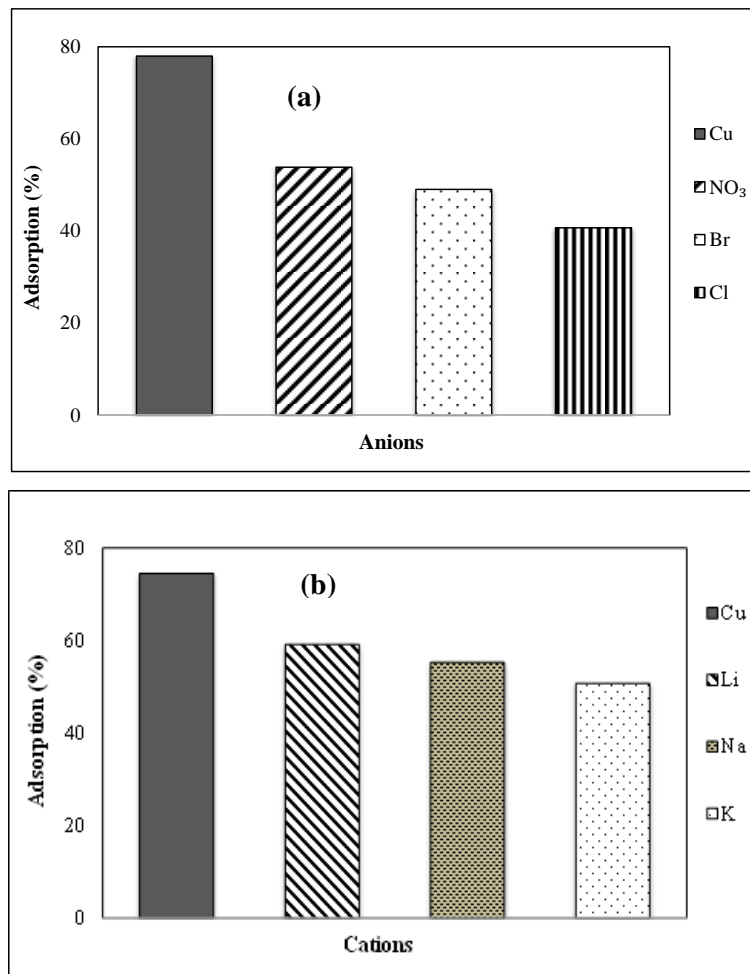


Figure 10: Effect of foreign ions on the Cu(II) adsorption by TMS (*T*: room temperature, pH = 4, *C*₀ = 250 mg L⁻¹, and *m* = 0.2 g mL⁻¹).

3.5. Thermodynamic study

The distribution coefficient *K_d* was calculated using Eq. (4). The plotting of ln*K_d* versus 1/*T* given in figure 11, shows a straight line with a correlation coefficient (*R*²) of 0.964. As it can be seen from figure 11, the distribution coefficient of Cu(II) adsorption by TMS increased with the increase in temperature, implying that high temperature was favorable for Cu(II) adsorption. The same phenomenon was observed by Nilchi et al. [36]. The calculated thermodynamic parameters (ΔH° , ΔS° , ΔG°) are summarized in Table 2 for different temperatures. The positive value of ΔH° indicates the endothermic nature of the adsorption process suggesting that the transfer of Cu(II) ions from the aqueous phase to the solid phase requires energy. The negative values

for the standard Gibbs free energy, ΔG° , suggest that the adsorption process is spontaneous and the degree of spontaneity of the reaction increases with increasing temperature. The positive value of ΔS° shows the increased randomness at the solid/solution interfaces during the adsorption of Cu(II) ions onto TMS. It also reflects the affinity of the TMS toward Cu(II) ions in aqueous solutions.

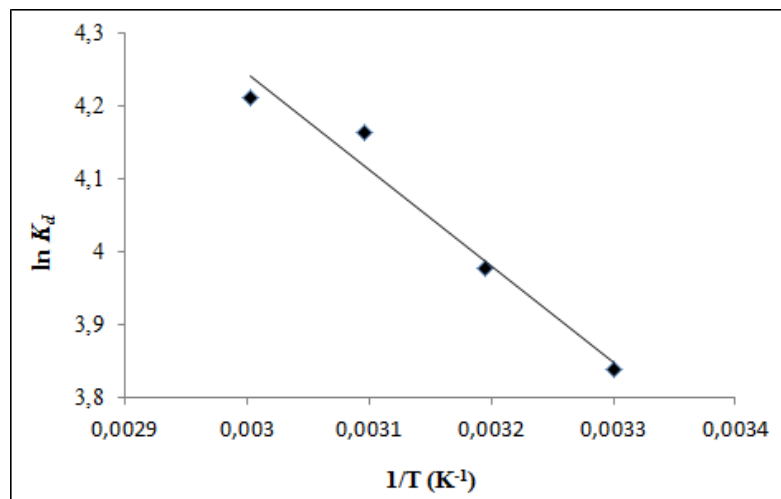


Figure 11: Effect of temperature on the distribution coefficients of Cu(II) on TMS (pH = 4, $C_0 = 250 \text{ mg L}^{-1}$, and $m = 0.2 \text{ g mL}^{-1}$).

Table 2: Thermodynamic parameters for the adsorption of Cu(II) onto TMS.

$T \text{ (K)}$	$\Delta G^\circ \text{ (kJ mol}^{-1}\text{)}$	$\Delta H^\circ \text{ (kJ mol}^{-1}\text{)}$	$\Delta S^\circ \text{ (J mol}^{-1}\text{)}$
303	-9.69	11.01	68.32
313	-10.38		
323	-11.06		
333	-11.74		

Conclusions

1. The present study investigated the ability of treated Martil sand (TMS) to adsorb Cu(II) from aqueous solution.
2. The operating parameters such as the contact time, particle size, solution pH, adsorbent dose, ionic strength and foreign ions were studied.
3. The amount of Cu(II) adsorbed onto TMS increased with the pH value.
4. The adsorption of Cu(II) is strongly dependent on the ionic strength.
5. Infrared spectra (IR) of TMS showed that the positions of the fundamental vibrations of the O–H and Si–O groups were influenced by the adsorbed Cu(II) cations.
6. The thermodynamic data indicated that the adsorption of Cu(II) on TMS is a spontaneous process.
7. The study indicates that the TMS is a good candidate as a low cost adsorbent to be used for the removal of heavy metals from wastewater.

References

1. Aksu Z., İšoğlu İ.A., *Process Biochem.* 40 (2005) 3031.
2. Rengaraj S., Yeon J-W, Kim Y., Yung Y., Ha Y-K, Kim W-H, *J. Hazard. Mater.* 143 (2007) 469.
3. Rao C.S. *Environmental Pollution Control Engineering*, Wiley, (1992).
4. Morcali M.H., Zeytuncu B., Baysal A., Akman S., Yucel O., *J. Environ. Chem. Eng.* 2 (2014) 1655.
5. Quki S.K., Kavannagh M., *Water Sc. Technol.* 39 (1999) 115.
6. Bhattacharyya K.G., Gupta S.S., *Sep. Purif. Technol.* 50 (2006) 388
7. Saeed A., Akhter M.W., Iqbal M., *Sep. Purif. Technol.* 45 (2005) 25.
8. Gupta V.K., Ali I., *Sep. Purif. Technol.* 18 (2000) 131.

9. Atun G., Hisarli G., *J. Colloid Interface Sci.* 228 (2000) 40.
10. Eren E., *J. Hazard. Mater.* 159 (2008) 235.
11. Rusch B., Hanna K., Humbert B., *Colloids and Surf. A: Physicochem. Eng. Aspects* 353 (2010) 172.
12. Nakamoto K., *Infrared Spectra of Inorganic and Coordination Compounds*, John Wiley and Sons, (1963).
13. Eren E., Asfin B., *J. Hazard. Mater.* 151 (2008) 682.
14. Xu Y, Axe L., *J. Colloid Interface Sci.* 282 (2005) 11.
15. Waseem M., Mustafa S., Naeem A., Koper G.J.M., Shah K.H., *Desalination* 277(2011) 221.
16. Al-Degs Y.S., El-Barghouthi M.I., Issa A.A., Khraisheh M.A., Walker G.M., *Water Res.* 40 (2006) 2645.
17. Khalil E.M.A., Elbatal F.H., Hamdy Y.M., Zidan H.M., Aziz M.S., Abdelghany A.M, *Physica B:* 405 (2010) 1294.
18. Sumasundaran P., Agar G.E., *J. Colloid Interface Sci.* 24 (1967) 433.
19. Fuerstenau M.C., Gutierrez G., Elgillani D.A., *Trans. AIME* 241 (1968) 319.
20. Sumasundaran P. *Encyclopedia of Surface and Colloid Science*, Taylor & Francis, (2006).
21. Sposito G. *The Surface Chemistry of Soils*, Oxford University Press, (1984).
22. Taqvi S.I.H., Hasany S.M., Bhangar M.I., *J. Hazard. Mater.* 141(2007) 37.
23. Wan Ngah W.S., Hanafiah M.A.K.M., *Biochem. Eng. J.* 39 (2008) 521.
24. Hossain M.A., Ngo H.H., Guo W.S., Setiadi T., *Bioresour. Technol.* 121 (2012) 386.
25. Jung J., Kim J.-A., Suh J.-K., Lee J.-M., Ryu S.-K., *Water Res.* 35 (2001) 937.
26. Shukla A., Zhang Y.H., Dubey P., Margrave J.L., Shukla S.S., *J. Hazard. Mater.* 95 (2002) 137.
27. El-Ashtoukhy E.-S.Z., Amin N.K. and Abdelwahab O., *Desalination* 223 (2008) 162.
28. Imamoglu M., Tekir O., *Desalination* 228 (2008) 108.
29. Zheng W., Li X.-M., Wang F., Yang Q., Deng P., Zeng G.-M., *J. Hazard. Mater.* 157 (2008) 490.
30. Han R., Zou W., Zhang Z., Shi J., Yang J., *J. Hazard. Mater.* B137 (2006) 384.
31. Phuengprasop T., Sittiwong J., Unob F., *J. Hazard. Mater.* 186 (2011) 502.
32. Jiang M., Jin X., Lu X., Chen Z., *Desalination* 252 (2010) 33.
33. Bohn H.L., McNeal B.L., O'Connor G.A., *Soil Chemistry*, Wiley, (1985).
34. Moyer B.A., Bonnesen P.V., Physical factors in anion separation, in: *Supramolecular Chemistry of Anions*, Wiley-VCH, (1997).
35. Esmadi F., Simm J., *Colloids Surf. A* 104 (1995) 265.
36. Nilchi A., Saberi R., Moradi M., Azizpour H., Zarghami R., *Chem. Eng. J.* 172 (2011) 572.

(2015) ; <http://www.jmaterenvirosci.com>